Control Strategy of High Power Converters with Synchronous Generator Characteristics for PMSG-based Wind Power Application

Yuzhi Zhang, Haoyan Liu, H. Alan Mantooth, Fellow, IEEE
NSF I/UCRC on GRid-connected Advanced Power Electronic Systems (GRAPES)
University of Arkansas, Fayetteville, AR 72701, U.S.A.
mantooth@uark.edu, yxz068@email.uark.edu

Abstract— **A virtual synchronous generator (VSG) control for high power permanent magnetic synchronous generators (PMSG) in wind power generation is investigated in this paper. A power factor correction (PFC) rectifier for each phase of the PMSG is designed to transform variable voltage and frequency of wind power into constant voltage DC power. The PFC boost inductor is replaced by a PMSG armature inductance to reduce the size and cost of the overall system. A three-phase inverter is used as a power interface to feed the generated wind power to the grid or load. By designing an excitation controller and a prime motor controller, the PMSG-based wind power interface can mimic a self-stabilization characteristic of synchronous generator which has rotor inertia, thus helping to improve the stability of wind power generation. Experimental results of the VSG inertia performance are illustrated, and the simulation results of traditional PQ and proposed VSG control are given and compared to validate the proposed converter topology and control algorithm.**

Keywords— virtual synchronous generator; permanent magnetic synchronous generator; power factor correction; Direct-Quadrature Frame; PQ control

I. INTRODUCTION

Today, more and more renewable energy such as fuel cell power, wind power, and solar power generation are connected to the grid. Compared with conventional power generation, renewable energy generation usually needs power converters as an interface to connect with the grid or load. Therefore, renewable energy generation has different steady states and dynamic characteristics from conventional power stations because of their own inherent characteristics, such as random and intermittent behavior. This poses potential risks to the secure and stable operation of the grid system and causes difficulty in the centralized power system management and control that has been reported in [1], [2] and [3].

Permanent magnetic synchronous generators (PMSGs) are prevalently used in wind power generation. Compared with the Doubly-Fed Induction Generator (DFIG), the PMSG has higher power density, better controllability, and a simple drive train structure. It does not need an excitation circuit and has much higher efficiency and reliability. There are two common rectification topologies widely used in PMSGs [4], [5]. One is a PMSG through a pulse-width modulation (PWM) rectifier to create a DC voltage for inverters. The structure of this topology is more complex, and needs protection to prevent excitation failure during faults. The other is a PMSG with an uncontrolled rectifier and boost converter to create a DC voltage for inverters. This topology needs an additional boost inductor for the boost converter and has a low power factor due to the uncontrolled rectifier. In order to overcome these drawbacks, a scheme of a Power Factor Correction (PFC) converter is applied in the paper to achieve a steady DC output voltage and unit power factor. It doesn't need an additional inductor, and thus saves on the cost and size of the system [6]. In the conventional method, the active and reactive power decoupling control or PQ control is widely used as a control strategy for inverters [7], [8]. Recently, virtual synchronous generators (VSGs) are under investigation for solar and DFIG-based wind power generation in micro-grids. However, most applications need additional energy storage equipment and rarely focus on the VSG application in high power PMSG [9], [10]. In this paper, a VSG controller is designed for PMSG-based high wind power generation to improve system stability performance such as self-regulation during power demand changes. The power converter combined with the designed VSG control algorithm makes PMSG-based wind power generation more reliable, efficient, and of higher quality to the grid or loads.

The outline of the paper is as follows. Section II describes the circuit diagram of PMSG-based wind power generation. Section III presents the control strategy design for the PFC and VSG control for inverters. Section IV shows the experimental results of the virtual inertia and the simulation results of conventional PQ and proposed VSG control for PMSGs. The conclusion and future work are given in the last section.

978-1-4673-9550-2/16/$31.00 ©2016 IEEE

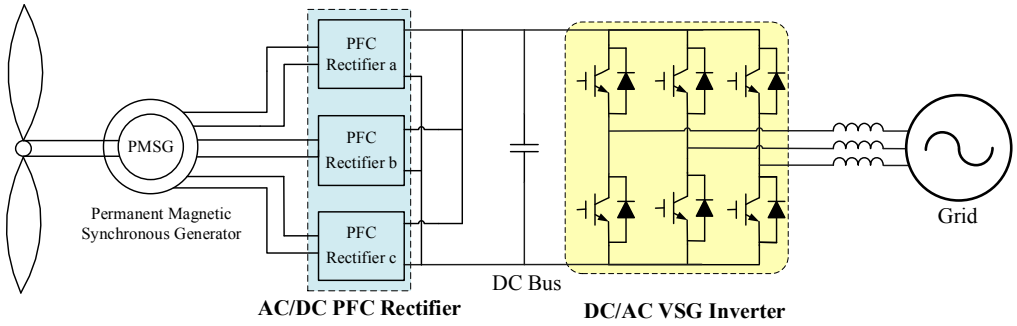

(a) PMSG-based wind power topology

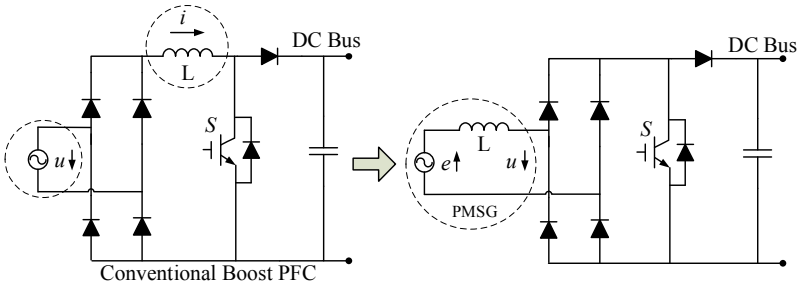

(b) PFC converter

Fig. 1. The scheme of proposed system.

II. THE CIRCUIT DIAGRAM OF THE PMSG-BASED WIND POWER GENERATION

As the proposed topology shown in Fig. 1, through the PFC rectifier which is diode rectifier combined with boost converter, the PMSG generates a steady DC bus and power factor is improved. The boost inductors are utilizing generator isolated coils. Therefore, the system size and cost can be further reduced. Three-phase inverter generates an AC voltage to connect with the grid or directly to the load. The three-phase inverter can be modular multi-level converter such as Neutral Point Clamped (NPC), Flying Capacitor (FC) or Series Connected H-Bridge (SCHB) converter. The detailed inverter control design for the proposed topology in Fig. 1 is presented in Section III.

III. PROPOSED CONTROL STRATEGY

A. Control Scheme of PFC rectifier

The PFC control scheme is shown in Fig. 2. PMSG with three generator coils are chosen as an example. There are two control loops. The voltage error between the DC reference value and DC bus voltage passes through PI control, and is then multiplied by the back electromotive force (EMF) phase of the generator to generate the reference current value. A sensorless control strategy is applied to get phase information of the winding back EMF estimation [11].

B. VSG control for inverter

The proposed VSG control scheme is based on the mathematical equations of a synchronous generator. The fifth-order Park transform equations of a synchronous generator are represented in Eqs. (1) and (2).

$$\begin{bmatrix} u_{\mathrm{d}} \\ u_{\mathrm{q}} \\ u_{\mathrm{e}} \\ u_{\mathrm{D}} \\ u_{\mathrm{Q}} \end{bmatrix} = p\begin{bmatrix} \psi_{\mathrm{d}} \\ \psi_{\mathrm{q}} \\ \psi_{\mathrm{e}} \\ \psi_{\mathrm{D}} \\ \psi_{\mathrm{Q}} \end{bmatrix} + \begin{bmatrix} R_{\mathrm{d}} & 0 & 0 & 0 & 0 \\ 0 & R_{\mathrm{q}} & 0 & 0 & 0 \\ 0 & 0 & R_{\mathrm{e}} & 0 & 0 \\ 0 & 0 & 0 & R_{\mathrm{D}} & 0 \\ 0 & 0 & 0 & 0 & R_{\mathrm{Q}} \end{bmatrix} \begin{bmatrix} -i_{\mathrm{d}} \\ -i_{\mathrm{q}} \\ i_{\mathrm{e}} \\ i_{\mathrm{D}} \\ i_{\mathrm{Q}} \end{bmatrix} + \begin{bmatrix} -\omega\psi_{\mathrm{q}} \\ \omega\psi_{\mathrm{d}} \\ 0 \\ 0 \\ 0 \end{bmatrix} \tag{1}$$

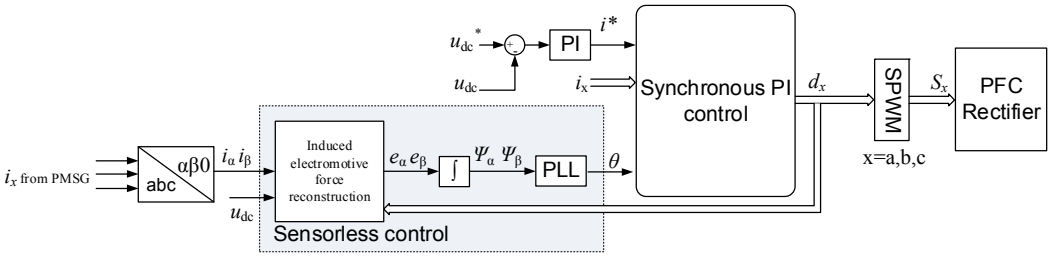

Fig. 2. The PFC control scheme for the PMSG.

$$\begin{bmatrix}\psi_{\mathrm{d}}\\ \psi_{\mathrm{q}}\\ \psi_{\mathrm{e}}\\ \psi_{\mathrm{D}}\\ \psi_{\mathrm{Q}}\end{bmatrix}=\begin{bmatrix}L_{\mathrm{d}} & 0 & M_{\mathrm{de}} & M_{\mathrm{dD}} & 0\\ 0 & L_{\mathrm{q}} & 0 & 0 & M_{\mathrm{qQ}}\\ M_{\mathrm{ed}} & 0 & L_{\mathrm{e}} & M_{\mathrm{eD}} & 0\\ M_{\mathrm{Dd}} & 0 & M_{\mathrm{De}} & L_{\mathrm{D}} & 0\\ 0 & M_{\mathrm{Qq}} & 0 & 0 & L_{\mathrm{Q}}\end{bmatrix}\begin{bmatrix}-i_{\mathrm{d}}\\ -i_{\mathrm{q}}\\ i_{\mathrm{e}}\\ i_{\mathrm{D}}\\ i_{\mathrm{Q}}\end{bmatrix} \tag{2}$$

where u is the winding voltage, ψ is the flux, ω is the synchronous angular velocity, p is number of pole-pairs. d, q, e, D, and Q are the d-axis winding, q-axis winding, excitation winding, d-axis damper winding, and q-axis damper winding, respectively.

The mechanical characteristic equation of the synchronous generator can be represented by Eq. (3).

$$\begin{cases} T_{\mathrm{m}}-T_{\mathrm{e}}-D\Delta\omega=\dfrac{P_{\mathrm{m}}}{\omega}-\dfrac{P_{\mathrm{e}}}{\omega}-D\Delta\omega=J\dfrac{d\Delta\omega}{dt} \\ \dfrac{d\theta}{dt}=\omega \end{cases} \tag{3}$$

where T_{m} and T_{e} are the mechanical and electromagnetic torque; P_{M} and P_{E} are mechanical power and electromagnetic power; D is a constant damping coefficient; $\Delta\omega=\omega-\omega_{\mathrm{n}}$, where $\Delta\omega$ is the electrical angular speed difference, ω and ω_{n} are the actual electrical angular speed and rated electric angular velocity, respectively.

The overall control block diagram of the VSG controller is shown in Fig. 3. It includes primary motion control and excitation control. The output active power P and reactive power Q can be represented by Eqs. (4) and (5), respectively. E and U are the inner potential and the bus voltage amplitude of the VSG, respectively. Φ is the power angle between E and U. In order to analyze the dynamic stability of VSG more accurately, this paper establishes a small-signal model of the VSG controller, then analyzes the stability of the system. Combining Eqs. (1), (2) and (3), the VSG small-signal model is given in Eq. (6). The coefficients of A, B, C, D, E, F, G are given in Eqs. (7), (8), (9), (10), (11), (12) and (13), respectively. The system stability with load power and inertia increases are shown in Figs. 4 (a) and (b), respectively. It shows a load power that is too high or an improper inertia value may lead to an unstable system. The small-signal equations can help to design the controller parameters as well.

$$P=\frac{U}{X_{\mathrm{eq}}}E\sin\phi \tag{4}$$

$$Q=\frac{U}{X_{\mathrm{eq}}}(E\cos\phi-U) \tag{5}$$

$$As^6\hat{\phi}+Bs^5\hat{\phi}+Cs^4\hat{\phi}+Ds^3\hat{\phi}+Es^2\hat{\phi}+Fs\hat{\phi}+G\hat{\phi}=0 \tag{6}$$

$$A=J\frac{\omega_{\mathrm{n}}}{n_{\mathrm{q}}} \tag{7}$$

$$B=\frac{m_{\mathrm{p}}}{2\pi n_{\mathrm{q}}}+2J\frac{\omega_{\mathrm{n}}\omega_{\mathrm{c}}}{Qn_{\mathrm{q}}} \tag{8}$$

$$C=\frac{m_{\mathrm{p}}\omega_{\mathrm{c}}}{Q\pi n_{\mathrm{q}}}+\frac{J\omega_{\mathrm{n}}}{n_{\mathrm{q}}}\left(\frac{\omega_{\mathrm{c}}^2}{Q^2}+2\omega_{\mathrm{c}}^2\right)+\frac{JU}{X_{\mathrm{eq}}}\cos(\phi)\omega_{\mathrm{c}}^2\omega_{\mathrm{n}} \tag{9}$$

$$D=\frac{m_{\mathrm{p}}(\omega_{\mathrm{p}}^2/Q^2+2\omega_{\mathrm{c}}^2)}{2\pi n_{\mathrm{q}}}+\frac{2\omega_{\mathrm{n}}J\omega_{\mathrm{c}}^3}{n_{\mathrm{q}}Q}+\frac{U\omega_{\mathrm{c}}^2m_{\mathrm{p}}\cos\phi}{2\pi X_{\mathrm{eq}}}+\frac{JU\cos\phi\omega_{\mathrm{c}}^2\omega_{\mathrm{n}}}{X_{\mathrm{eq}}Q} \tag{10}$$

$$E=\frac{m_{\mathrm{p}}\omega_{\mathrm{c}}^3}{n_{\mathrm{q}}\pi Q}+\frac{J\omega_{\mathrm{n}}\omega_{\mathrm{c}}^4}{n_{\mathrm{q}}}+\frac{m_{\mathrm{p}}U\omega_{\mathrm{c}}^2\cos\phi}{2X_{\mathrm{eq}}Q\pi}+\frac{JU\omega_{\mathrm{n}}\omega_{\mathrm{c}}^2\cos\phi}{X_{\mathrm{eq}}}+\frac{240U\omega_{\mathrm{c}}^2\cos\phi}{X_{\mathrm{eq}}n_{\mathrm{q}}} \tag{11}$$

$$F=\frac{m_{\mathrm{p}}\omega_{\mathrm{c}}^4}{2\pi n_{\mathrm{q}}}+\frac{240UQ\cos\phi\omega_{\mathrm{c}}^3}{n_{\mathrm{q}}X_{\mathrm{eq}}}+\frac{m_{\mathrm{p}}U\omega_{\mathrm{c}}^4\cos\phi}{2\pi X_{\mathrm{eq}}} \tag{12}$$

$$G=\frac{240U^2\omega_{\mathrm{c}}^4}{X_{\mathrm{eq}}{}^2}+\frac{240UQ\cos\phi\omega_{\mathrm{c}}^3}{X_{\mathrm{eq}}n_{\mathrm{q}}} \tag{13}$$

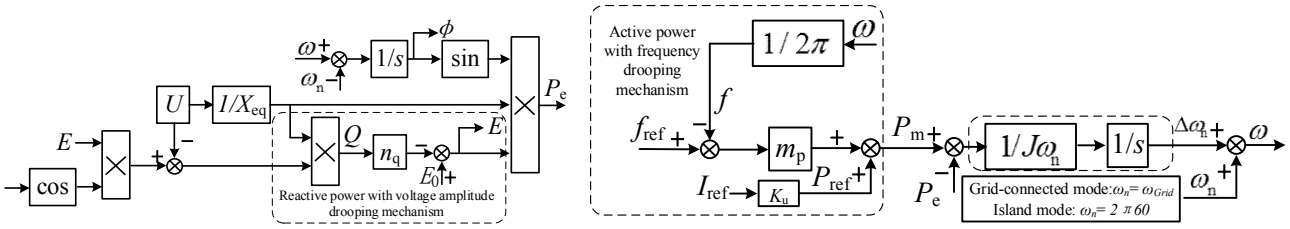

Fig. 3. Diagram of VSG controller for PMSG.

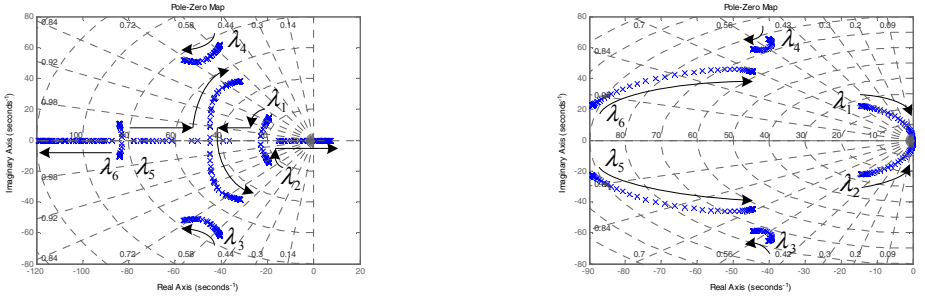

(a) Eigenvalue migration with power angle increased (b) Eigenvalue migration with inertia increased

Fig. 4. Simulation results of small-signal model.

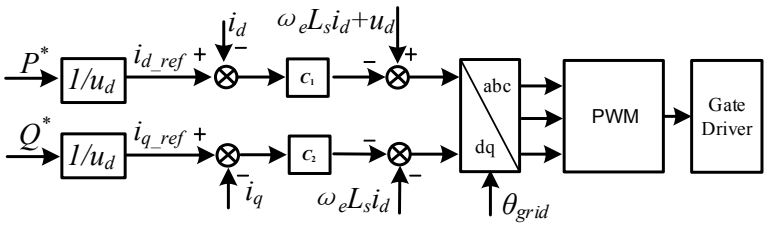

Fig. 5. Conventional PQ control for PMSG-based wind power generation.

C. Conventional PQ control

To compare with the proposed VSG control for PMSG, the conventional PQ control is given in Fig. 5 [8], [12]. The decouple control can be determined by Eqs. (14) and (15).

$$L_s \, di_d / dt = u_d - S_d - R i_d + \omega_e L_s i_q \quad (14)$$

$$L_s \, di_q / dt = u_q - S_q - R i_q - \omega_e L_s i_d \quad (15)$$

where i_d, i_q, u_d and u_q are the grid currents and voltages in the d, q axis. L_s and R are the inductance and resistance from the grid-side. ω_e is the electrical speed. S_d, S_q are the inverter output voltages.

IV. SIMULATION AND EXPERIMENTAL VERIFICATION

In order to verify the proposed VSG control for the PMSG-based wind power generation, both experimental testing and simulations are conducted. The VSG rotor inertia experimental results and overall system simulation results are shown in Fig. 6 and Fig. 7, respectively. Compared with Fig. 6(a), Fig. 6(b) shows that the dynamic response of the system changes faster due to the smaller inertia J. This phenomenon is the same as the actual synchronous generator. Therefore, the dynamic response performance of the system can be adjusted by changing the virtual inertia parameter in the controller to get a better dynamic response of the system.

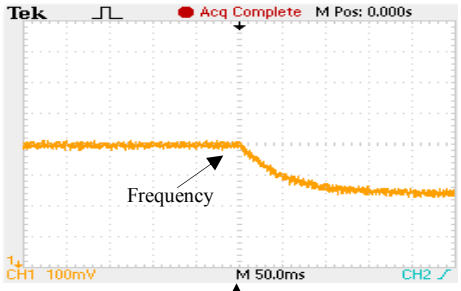

(a) J=1 kg·m^2

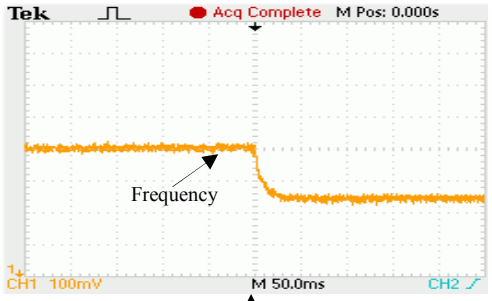

(b) J=0.1 kg·m^2

Fig. 6. Frequency responses of different rotary inertia.

Fig. 7(a) and (b) show the simulation results of step-up active power. With the proposed VSG control in PMSG, the output active power achieves a reference value 0.275 MW within 1.5 ms. However, PQ control requires a longer settling time of 5 ms and has higher coupled reactive power Q during the transition time as shown in Fig. 7(b). This is detrimental for inverter voltage stability. Similarly, during the step-up reactive power, Fig. 7(c) and (d) show the VSG control has a shorter response time, and the coupled active power P is much smaller than the PQ control.

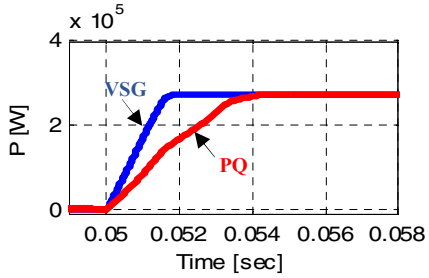

(a) Actvie power P_{ref}=0.275 MW

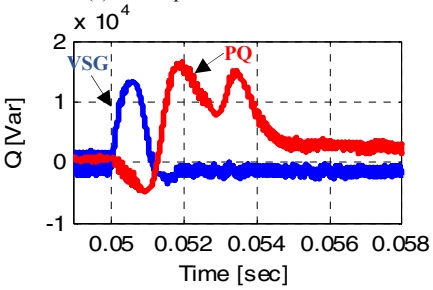

(b) Coupled reactive power Q

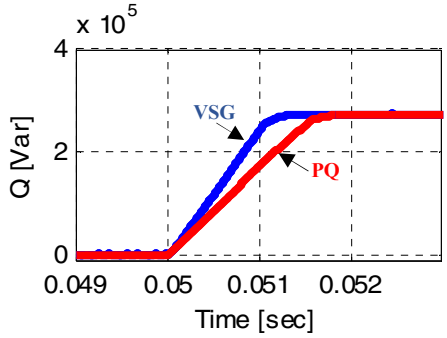

(c) Reactive power Q_{ref}=0.275 MVar

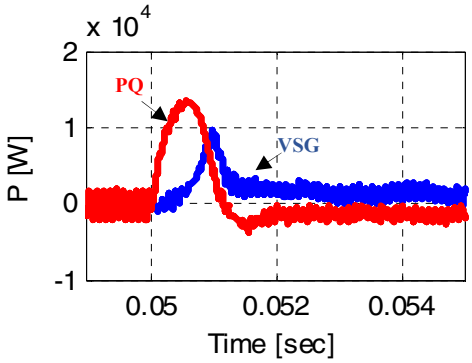

(d) Coupled active power P

Fig. 7. Simulation results comparison between conventional PQ and proposed VSG control.

V. SUMMARY AND FUTURE WORK

This paper presents virtual synchronous generator control for the PMSG-based wind power generation. The excitation and prime motor controllers are designed. The small-signal modeling of synchronous generator is built to optimize the controller parameters. Compared with the actual synchronous generator, the VSG parameters are much easier to design. Compared with the conventional PQ control, the VSG control has better transient dynamics and power decoupled performance in a PMSG-based wind system. Both simulation and experimental results have verified that the proposed topology and its optimized control strategy work as predicted. A more detailed description of the control algorithm and test results will be provided in future work.

ACKNOWLEDGMENTS

Special appreciation goes to the National Science Foundation Industry/University Cooperative Research Center on GRid-connected Advanced Power Electronic Systems (GRAPES) members, the sponsors of this work.

REFERENCES

[1] Jian Xu; Siyang Liao; Yuanzhang Sun; Xi-Yuan Ma; Wenzhong Gao; Xiaomin Li; Junhe Gu; Jianxun Dong; Mi Zhou, "An Isolated Industrial Power System Driven by Wind-Coal Power for Aluminum Productions: A Case Study of Frequency Control," *Power Systems, IEEE Transactions on* , vol.30, no.1, pp.471,483, Jan. 2015.

[2] Kai Tan; Huang, A.Q.; Martin, A., "Development of solid state arc-free socket for DC distribution system," in *Applied Power Electronics Conference and Exposition (APEC), 2014 Twenty-Ninth Annual IEEE* , vol., no., pp.2300-2305, 16-20 March 2014.

[3] Ozkan, M.B.; Karagoz, P., "A Novel Wind Power Forecast Model: Statistical Hybrid Wind Power Forecast Technique (SHWIP)," *Industrial Informatics, IEEE Transactions on* , vol.11, no.2, pp.375,387, April 2015.

[4] Shih-Yu Yang; Yuan-Kang Wu; Huei-Jeng Lin, "The direct torque control of the PMSG based windturbine with two level voltage source converter," *Automatic Control Conference (CACS), 2014 CACS International* , vol., no., pp.39,44, 26-28 Nov. 2014.

[5] Shao Zhang; King-Jet Tseng; Vilathgamuwa, D.M.; Trong Duy Nguyen; Xiao-Yu Wang, "Design of a Robust Grid Interface System for PMSG-Based Wind Turbine Generators," *Industrial Electronics, IEEE Transactions on* , vol.58, no.1, pp.316,328, Jan. 2011.

[6] Lifei Liu; Yingtao Ma; Jianyun Chai; Xudong Sun, "Cascaded single phase PFC rectifier pair for permanent magnet wind generation system," *Electrical Machines and Systems, 2008. ICEMS 2008. International Conference on* , vol., no., pp.2516,2520, 17-20 Oct. 2008.

[7] Lee, C-.T.; Chu, C-.C.; Cheng, P-.T., "A New Droop Control Method for the Autonomous Operation of Distributed Energy Resource Interface Converters," *Power Electronics, IEEE Transactions on* , vol.28, no.4, pp.1980,1993, April 2013.

[8] Adhikari, S.; Fangxing Li, "Coordinated V-f and P-Q Control of Solar Photovoltaic Generators With MPPT and Battery Storage in Microgrids," *Smart Grid, IEEE Transactions on* , vol.5, no.3, pp.1270,1281, May 2014.

[9] Wang, S.; Hu, J.; Yuan, X., "Virtual Synchronous Control for Grid-Connected DFIG-Based Wind Turbines," *Emerging and Selected Topics in Power Electronics, IEEE Journal of* , vol.PP, no.99, pp.1,1.

[10] Albu, M.; Visscher, K.; Creanga, D.; Nechifor, A.; Golovanov, N., "Storage selection for DG applications containing virtual synchronous generators," *PowerTech, 2009 IEEE Bucharest* , vol., no., pp.1,6, June 28 2009-July 2 2009.

[11] Yingtao Ma; Xudong Sun; Jianyun Chai, "Three-phase PFC rectifier with sensorless control for PMSG wind generation system," *Electrical Machines and Systems (ICEMS), 2011 International Conference on* , vol., no., pp.1,4, 20-23 Aug. 2011.

[12] Kai Tan; Qiongxuan Ge; Zhenggang Yin; Congwei Liu; Yaohua Li, "The optimal control strategy for rectifier side of low switching frequency back-to-back converter," in *Applied Power Electronics Conference and Exposition (APEC), 2010 Twenty-Fifth Annual IEEE* , vol., no., pp.1419-1423, 21-25 Feb. 2010.